**ADVANCED
OPTICAL
MATERIALS**

Supporting Information

High-Purity Hybrid Structural Colors by Enhancing Optical Absorption of Organic Dyes in Resonant Cavity

Zhengmei Yang, Chengang Ji, Qingyu Cui, and Lingjie Jay Guo*

High-purity hybrid structural colors by enhancing optical absorption of organic dyes in resonant cavity

Zhengmei Yang,[1,2,#] Chengang Ji,[1,#] Qingyu Cui,[1] and L. Jay Guo[1,*]

[1] Department of Electrical Engineering and Computer Science, University of Michigan, Ann Arbor, Michigan 48109, USA

[2] School of Physics and Electronics, State Key Laboratory of Advanced Design and Manufacturing for Vehicle Body, Hunan University, Changsha 410082, China

[#] These authors contribute equally to this work.

* Corresponding author: guo@umich.edu
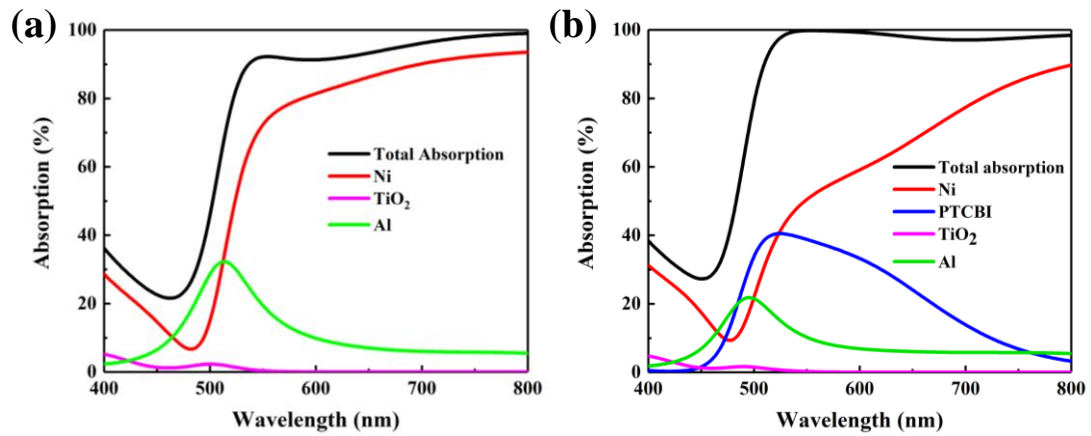
Figure S1. (a, b) Total absorption spectra and separate absorption in each layer for the blue color filters employing the single Ni absorber (a) and the Ni-PTCBI composite absorber (b), respectively. Obviously, the strong optical absorption outside the blue color range occurs mainly inside the absorber layers for both of these two devices. The absorption of Ni in the Ni-PTCBI composite based blue color filter is much less than that of Ni in the filter employing the single Ni absorber. Therefore, it is the PTCBI film that leads to the enhanced absorption of the device based on the Ni-PTCBI composite absorber.
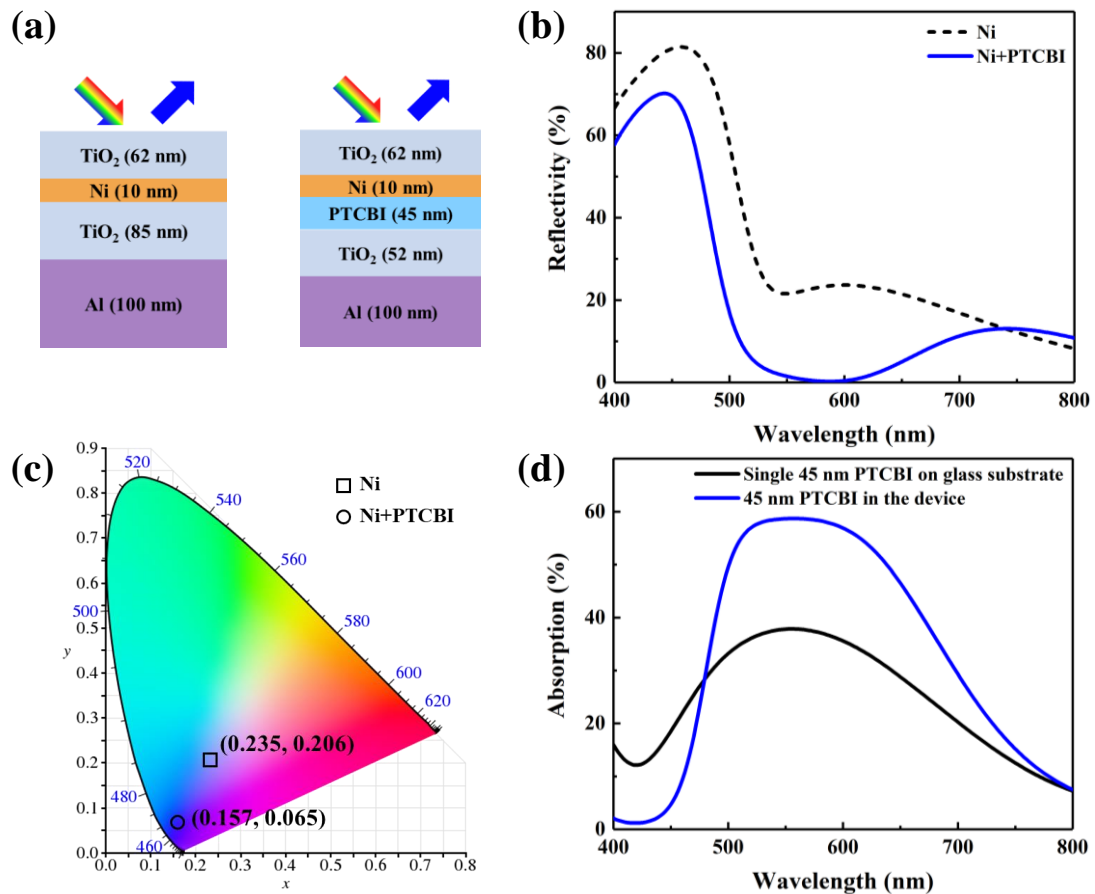
Figure S2. (a) The schematic diagrams of the designed blue reflective color filters employing a single 10 nm-thick Ni absorber (left) and a Ni-PTCBI composite absorber (right), respectively. All the thickness of the spacer layer (85 nm-thick TiO_2 for the left device; 45 nm-thick PTCBI and 52 nm-thick TiO_2 for the right device) corresponds to the half-wave optical thickness of the wavelength of 470 nm. (b) Comparison of the simulated reflection spectra of these two devices. The light absorption in the unwanted wavelength range of 500 ~ 800 nm is significantly enhanced by using the Ni-PTCBI composite absorber compared with the device using single Ni absorber. (c) The calculated color coordinates from the simulated reflection spectra shown in (b) on the CIE 1931 chromaticity diagram. The color filter based on the Ni-PTCBI composite absorber exhibits much improved color purity than the device using the single Ni absorber, and its location is also very close to the standard blue point. (d) Comparison of the absorption spectrum of PTCBI in the designed blue device to the absorption profile of a single 45 nm PTCBI on a glass substrate. Compared to the single PTCBI film on a glass substrate, the absorption of the PTCBI layer in the structural color at long wavelengths is largely enhanced due to the F-P cavity resonance excited in the structure. Meanwhile, the absorption at short wavelengths is also reduced. As the thickness of

the Ni absorber in the structural color here decreases from 15 nm to 10 nm compared to the design discussed in the main text, the absorption enhancement of the PTCBI at long wavelengths is even more obvious.
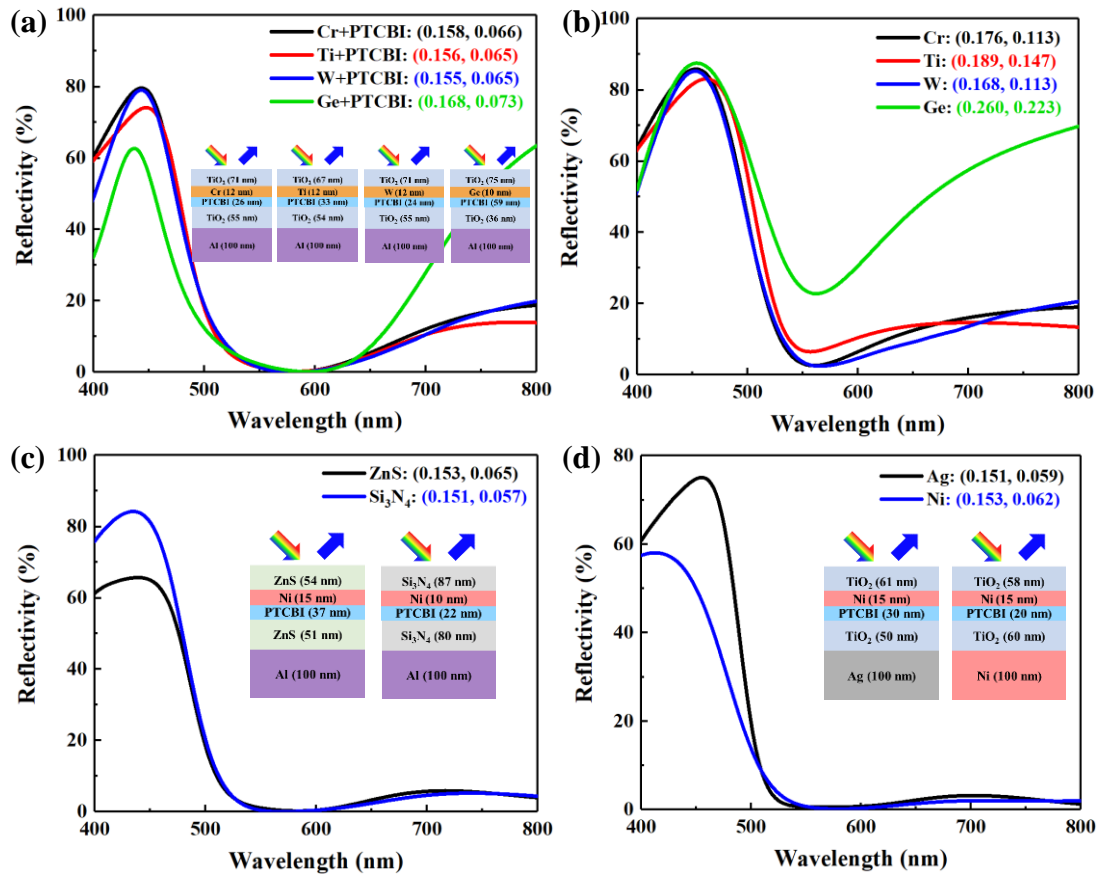
Figure S3. (a) The simulated reflection spectra of the designed blue reflective colors generating by placing the blue colored dye below different absorbing materials, including Cr, Ti, W, and Ge. (b) The simulated reflection spectra of the blue color filters based on single absorbing materials. According to their calculated chromaticity coordinates on the CIE 1931 color space, the blue color devices based on composite absorbers with additional dye layers exhibit much improved color purity compared to the color filters using a single absorber layer. (c) The simulated reflection spectra of two blue reflective color filters employing ZnS and Si_3N_4 dielectric materials, respectively. (d) The simulated reflection spectra of two blue color filters with different reflective layers, including Ag and Ni. The insets show the detailed structural parameters.
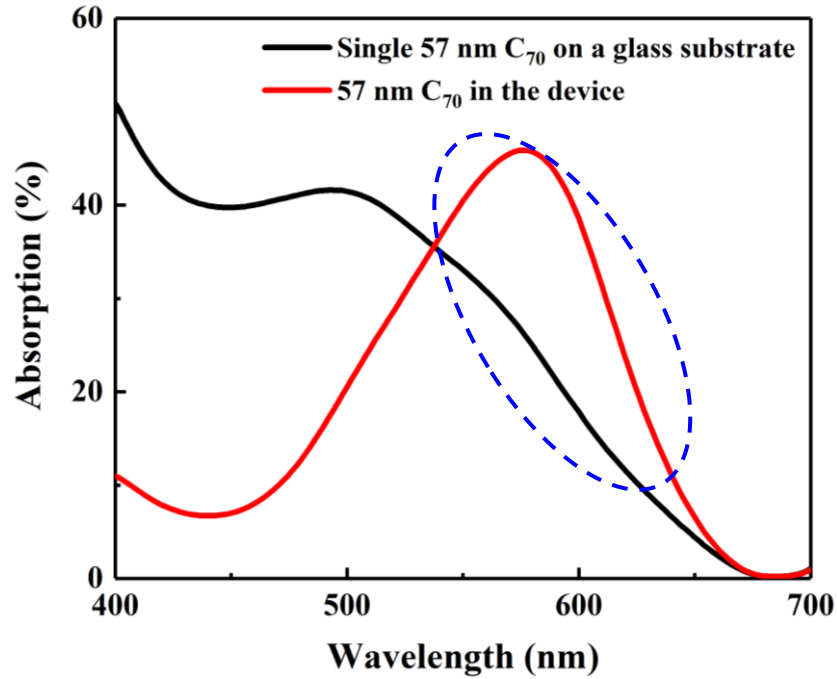
Figure S4. Comparison of the absorption of C_{70} in the red color device based on the Ge-C_{70} composite absorber to that of a single C_{70} layer on a glass substrate.

Figure S4 compares the absorption spectra of the C_{70} layer in the red color device based on the Ge-C_{70} composite absorber and a single C_{70} on a glass substrate. It can be seen that the absorption in the wavelength range of 540 ~ 650 nm as highlighted by the blue dotted circle is significantly enhanced due to the strongly enhanced electric field caused by the F-P cavity resonance. However, the C_{70} layer in the red color device exhibits lower absorption below 540 nm than that on the glass substrate, which is attributed to the high loss of the thin Ge film used in the asymmetric F-P cavity. The absorption in the 20 nm-thick Ge layer is too strong, which weakens the absorption contribution from the red dye to the final color purity of the red color device. However, the absorption contribution from the red dye can be clearly validated by reducing the thickness of Ge or replacing Ge with a less absorptive Ag layer. As illustrated in Figure S5a-S5b, the color filter based on a Ge (8 nm)-C_{70} composite absorber still exhibits much improved color purity than the structure based on a single

Ge (8 nm) layer, and the light absorption of the C_{70} layer at most unwanted wavelengths is enhanced after being integrated into the F-P resonator due to the reduced absorption in the thinner Ge layer. The results for the red color filter employing Ag-C_{70} composite absorber shown in Figure S5c-S5d further indicate that the color purity of the red reflective color can be significantly improved by the added red dye film, where the light absorption outside the red color range can be greatly enhanced by the strong F-P cavity resonance.
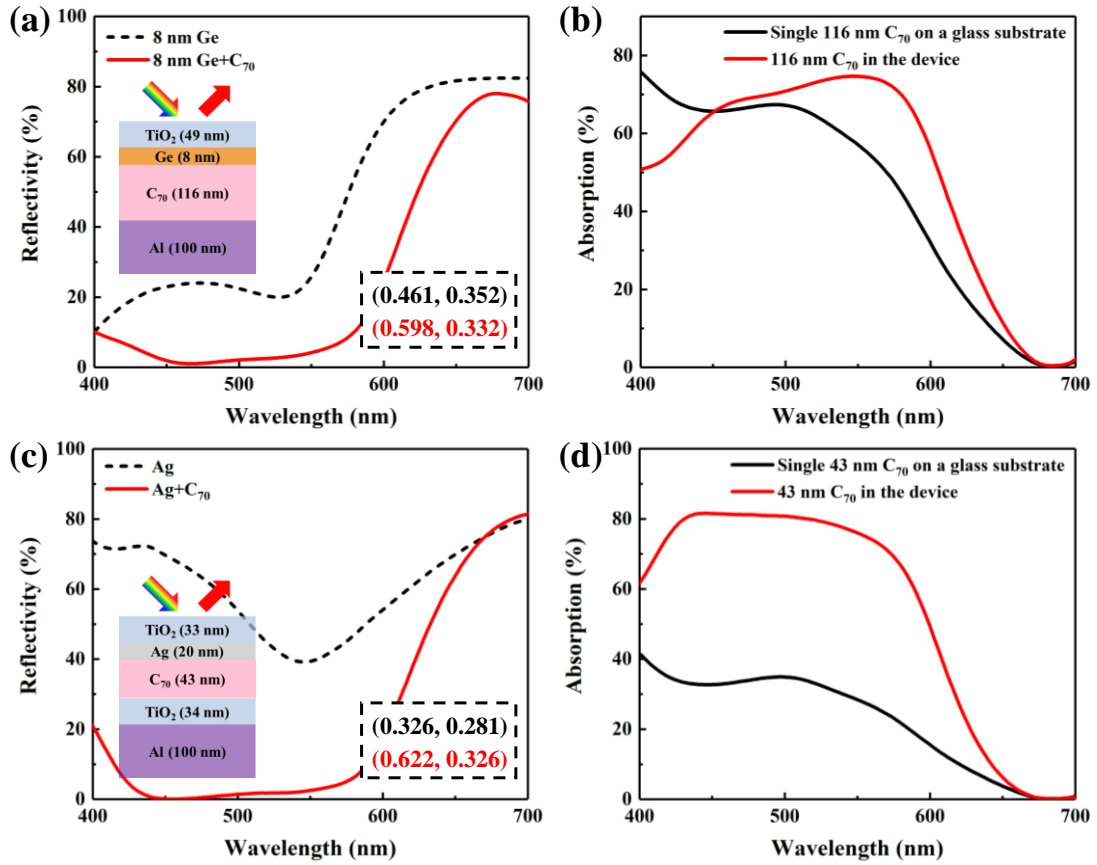
Figure S5. (a, c) Comparison of the simulated reflection spectra of red color filters based on Ge (8 nm)-C_{70} (a) and Ag-C_{70} (c) composite absorbers to the reflection profiles of those based on single lossy medium absorbers. The corresponding chromaticity coordinates on the CIE 1931 color space are shown in the dotted boxes. The schematic diagrams of the devices based on composite absorbers are shown in the insets. (b, d) Comparison of the absorption spectra of C_{70} in the Ge- (b) and Ag- (d) based devices to the absorption profiles of single C_{70} films on the glass substrate.
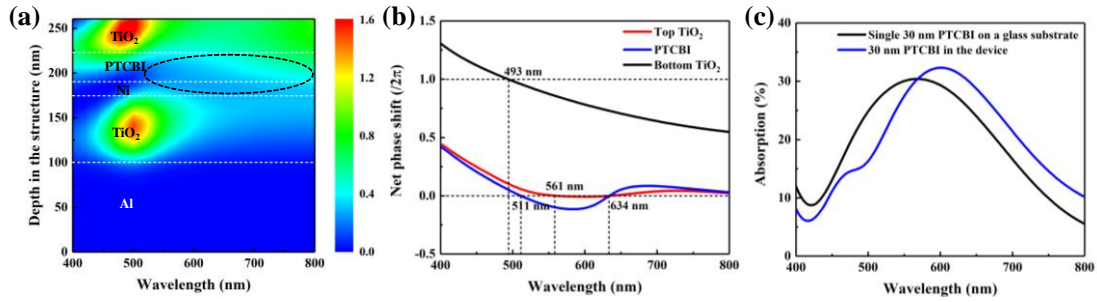
Figure S6. (a) The electric field distribution inside the designed blue color filter based on the PTCBI-Ni composite absorber as a function of wavelength. (b) The calculated net phase shifts within the PTCBI, top and bottom TiO₂ layers of the device. (c) Comparison of the absorption spectra of PTCBI before and after being integrated into the blue colored structure.

The electric filed distribution inside the whole structure of the proposed blue color filter based on the PTCBI-Ni composite absorber as a function of the wavelength is calculated and displayed in Figure S6a. Similarly, the strong electric field at wavelength >500 nm (the black dotted circle) and the weak electric field at short wavelengths in the PTCBI-Ni composite absorber directly result in the significant light absorption outside the blue color range and the high reflectance of the blue color, respectively. In Figure S6b, the net phase shifts inside the PTCBI, top and bottom TiO₂ layers of the device are plotted to reveal the resonant locations. As illustrated by the black curve, a F-P cavity resonance is excited within the bottom TiO₂ layer (@493 nm) when the net phase shift is equal to a multiple of 2π, which is consistent with the location of the strongly confined electric field in this layer. Multiple AR resonances are excited within the PTCBI layer (@511 nm and @634 nm, the blue curve) and the top TiO₂ overlayer (@561 nm and @634 nm, the red curve), effectively suppressing the broadband reflection at the unwanted wavelengths (500 ~ 800 nm) with the enhanced light absorption in the PTCBI-Ni composite absorber, which function together leading to a perfect absorption peak at the wavelength of 554 nm. Comparing the absorption of the PTCBI layer in the device and that of a single PTCBI on the glass substrate as shown in Figure S6c, the absorption at long wavelengths of the dye layer in the color filter is enhanced by the strong AR resonances, which improves the purity of the targeted reflective color.
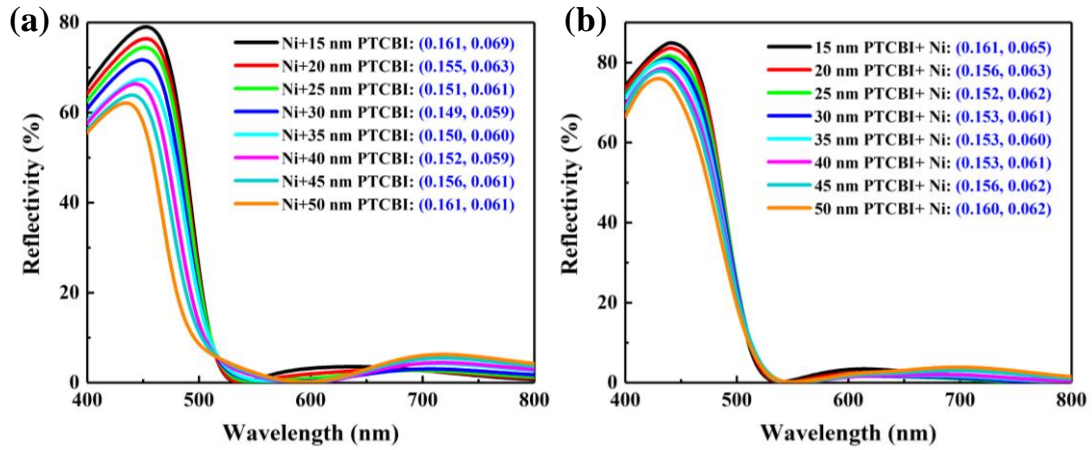
Figure S7. (a, b) The simulated reflection spectra of the optimized blue reflective colors generated by placing PTCBI with varied thickness below (a) or above (b) the 15 nm-thick Ni absorber layer. Their corresponding chromaticity coordinates on the CIE 1931 color space are also calculated. In both cases, the peak reflection intensity gradually decreased as the thickness of PTCBI increases from 15 nm to 50 nm. Besides, the color coordinate gradually moves toward to and then away from the standard blue point (0.150, 0.060). Highly pure blue reflective colors can be obtained with the thickness of PTCBI in the range of 20 ~ 45 nm.
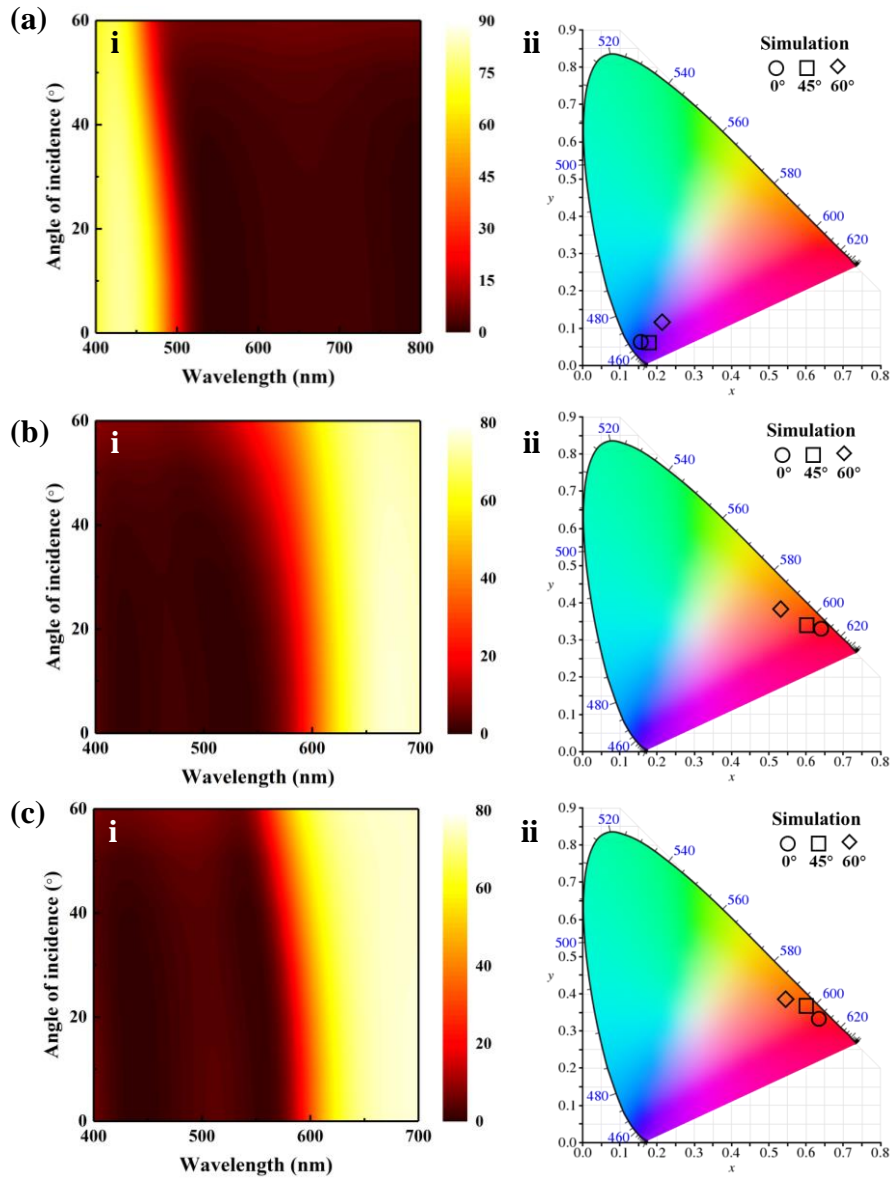
Figure S8. (a-c) (i) The simulated angle-resolved reflection spectra of the proposed high-purity reflective structural color filters under unpolarized light incidence, and (ii) the visualizations of the color change with the incident angle on the CIE 1931 chromaticity diagrams. They are (a) the blue color filter employing the PTCBI-Ni composite absorber, (b) the red color filters employing the Ge-C_{70} (b) and C_{70}-Ge (c) composite absorber, respectively.
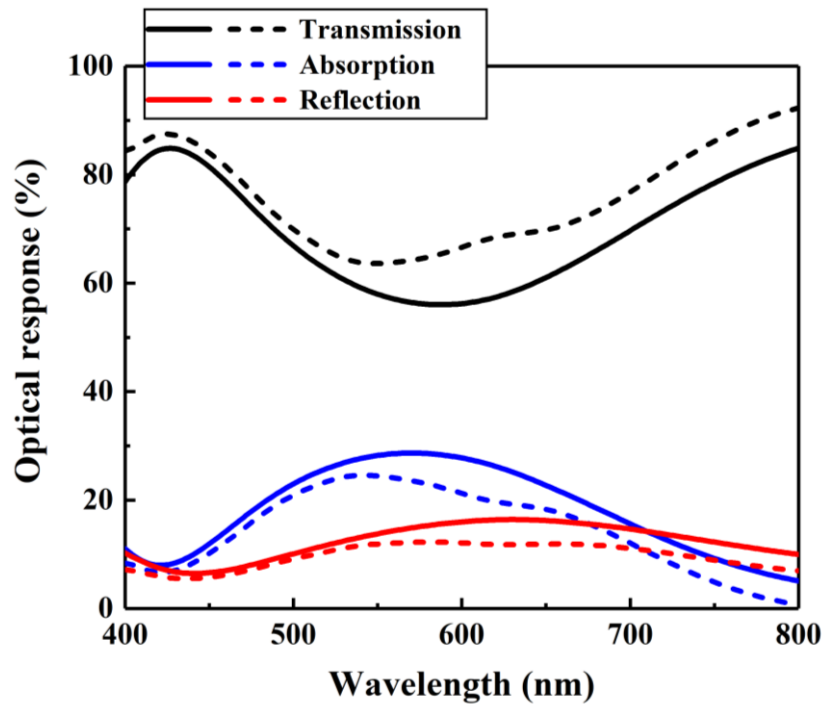
Figure S9. The simulated reflection/transmission/absorption spectra of a 27 nm-thick PTCBI film on a glass substrate before (the solid curves) and after (the dashed curves) the accelerated UV exposure test for 15 days.
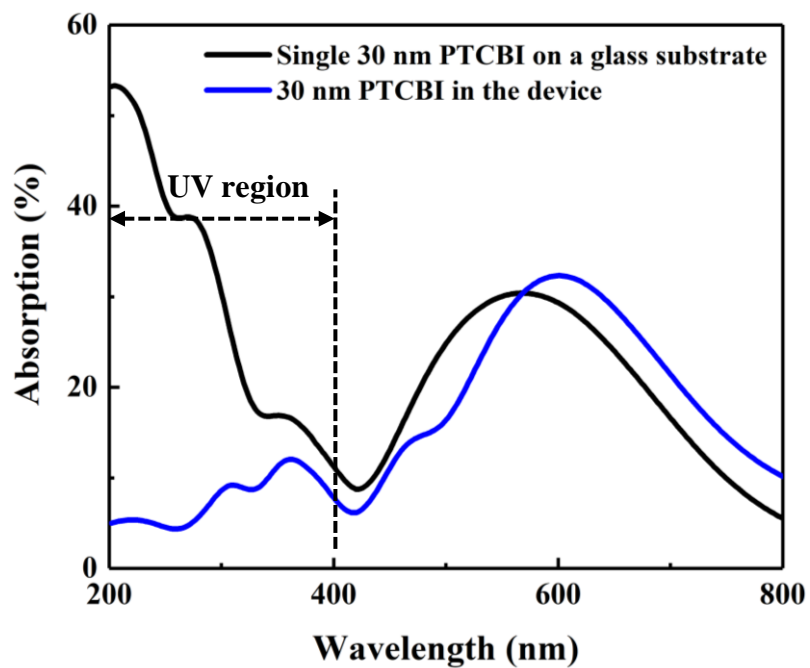
Figure S10. Comparison of the simulated UV-visible absorption spectrum of the PTCBI layer in the proposed blue color device based on the PTCBI-Ni composite absorber to the absorption profile of a single 30 nm PTCBI on a glass substrate.
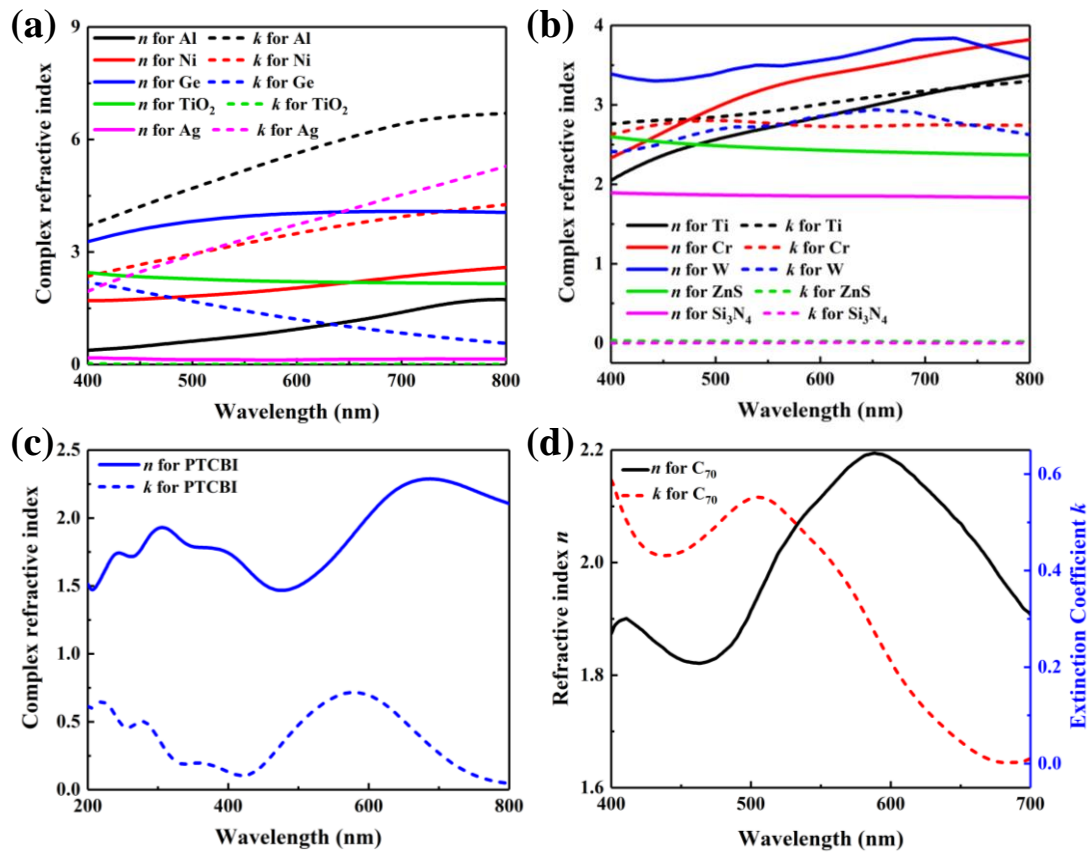
Figure S11. (a-c) The measured refractive indices of Al, Ag, Ti, Cr, W, Ni, Ge, TiO$_2$, ZnS, Si$_3$N$_4$, and PTCBI using a spectroscopic ellipsometer (M-2000, J. A. Woollam). (d) The optical constant of C$_{70}$ fullerene taken from the Ref. [52] in the main text.
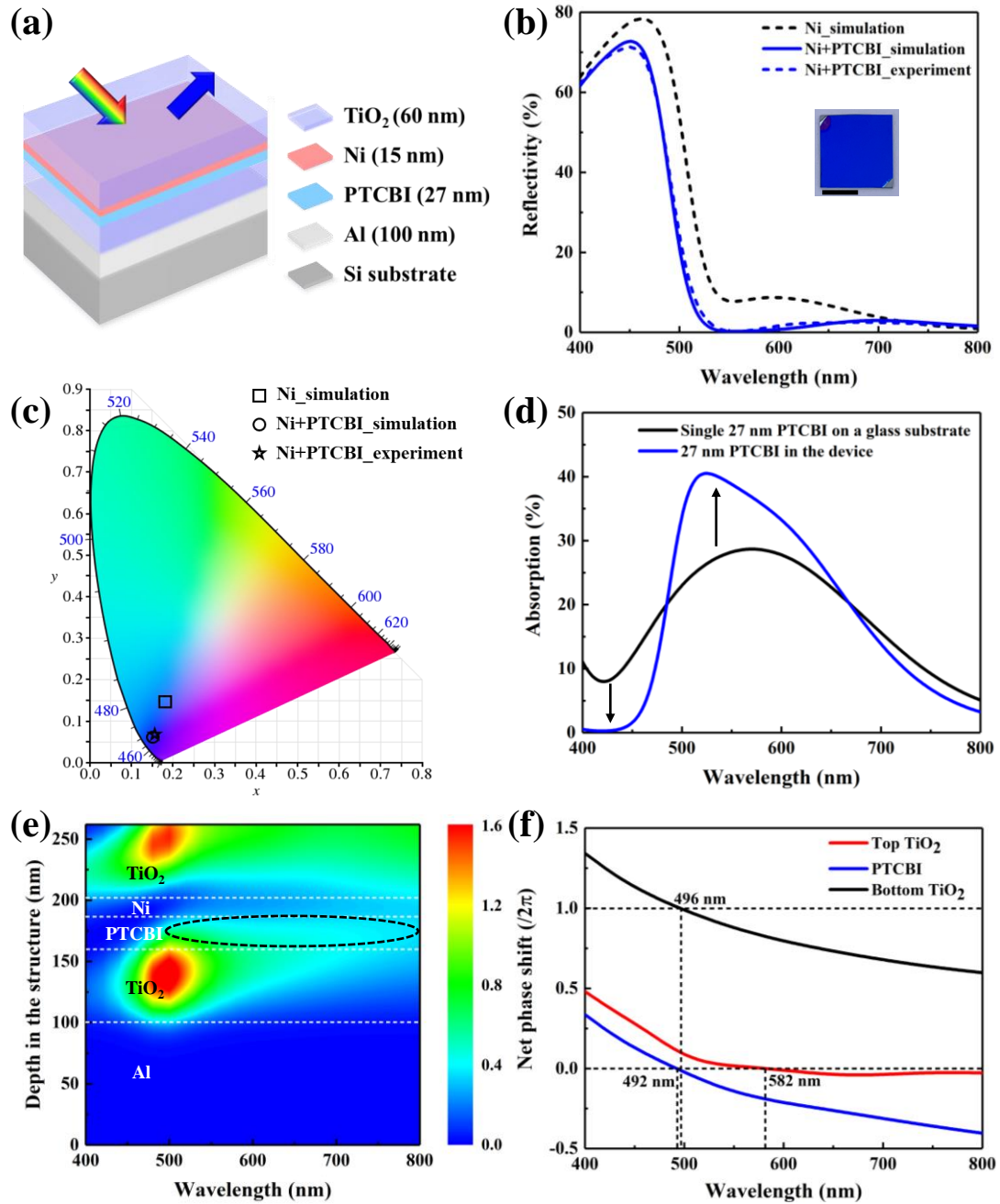
Figure 1. (a) The schematic diagram of the proposed high-purity blue reflective color filter using a Ni-PTCBI composite absorber. (b) Comparison of the simulated and measured reflection spectra of blue color filters employing the single Ni absorber and the Ni-PTCBI composite absorber. The inset shows a photograph of the fabricated blue color device on a silicon substrate (Scale bar: 1.0 cm). (c) The calculated color coordinates corresponding to all the reflection spectra shown in (b) on the CIE 1931 chromaticity diagram. (d) Comparison of the absorption spectrum of the PTCBI layer in the proposed blue color device to the absorption profile of a single 27 nm PTCBI on a glass substrate. (e) The wavelength-dependent electric field distribution inside the whole structure

of the proposed blue color filter employing the Ni-PTCBI composite absorber. (f) Calculated net phase shifts in the PTCBI, top and bottom TiO_2 layers as a function of the wavelength for the device.
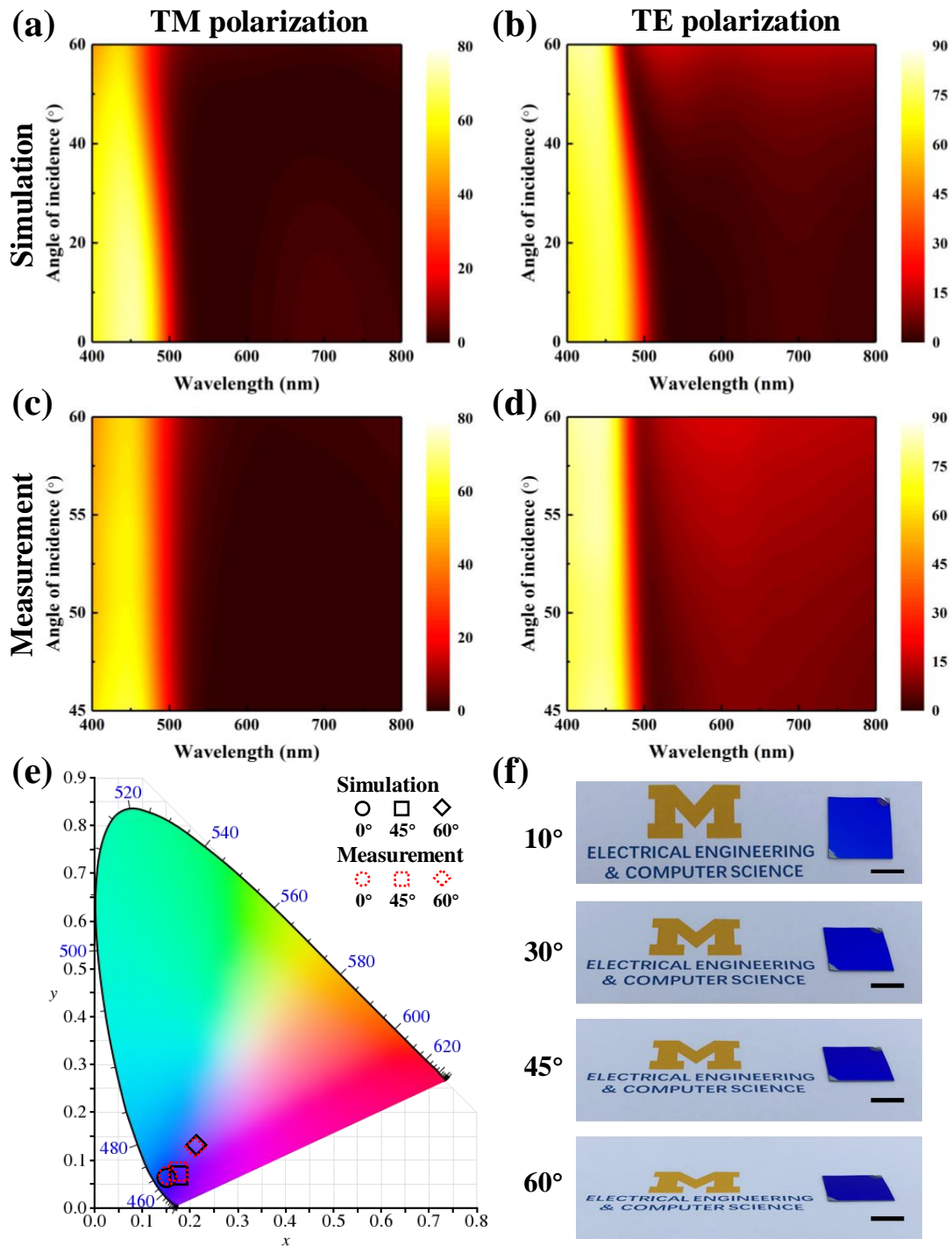
Figure 4. (a) and (b) The simulated angle-resolved reflection spectra of the proposed blue color filter employing the Ni-PTCBI composite absorber under TM and TE polarizations. (c) and (d) Measured angular behaviors corresponding to those in (a) and (b). (e) Visualization of the color change with the incident angle on the CIE 1931 chromaticity diagram. (f) Photographic images of the fabricated blue color device taken with the ambient light at oblique incidence of 10°, 30°, 45° and 60°. The scale bars are 1.0 cm.
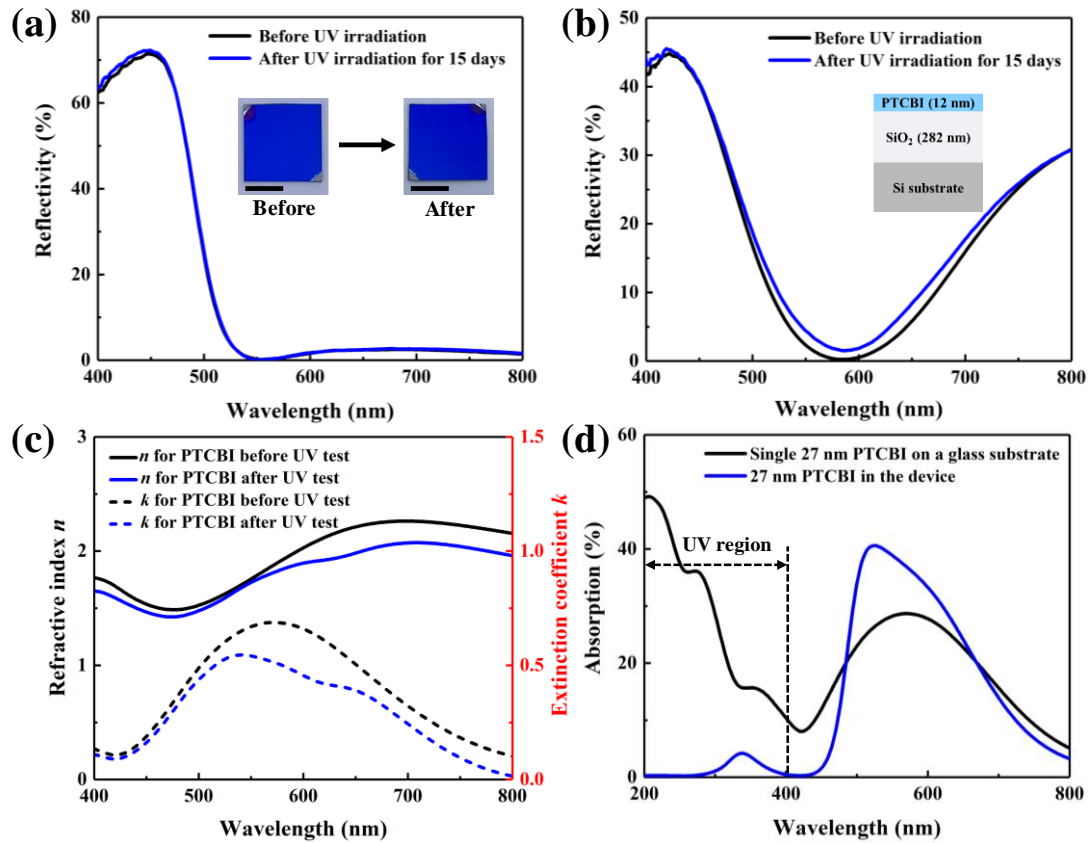
Figure 5. (a, b) Comparison of the measured reflection spectra of the fabricated blue color filter based on the Ni-PTCBI composite absorber (a) and a reference sample (b) before and after UV irradiation for 15 days. The insets in (a) display the optical images of the blue device before and after UV test (Scale bar: 1.0 cm). The schematic view of the reference sample shown as the inset in (b). (c) Comparison of the measured complex refractive indices of PTCBI (in the reference sample) before and after UV test. (d) Comparison of the simulated UV-visible absorption spectra of PTCBI before and after being integrated into the blue colored structure.